



Profiling of Metabolites of *Bacillus* spp. and Their Application in Sustainable Plant Growth Promotion and Biocontrol

Izzah Shahid^{1,2,3}, Jun Han³, Sharoon Hanoq², Kauser A. Malik²,
Christoph H. Borchers^{3,4,5,6} and Samina Mehnaz^{2*}

¹ Department of Biotechnology, Faculty of Life Sciences, University of Central Punjab, Lahore, Pakistan, ² School of Life Sciences, Forman Christian College (A Chartered University), Lahore, Pakistan, ³ University of Victoria - Genome BC Proteomics Center, University of Victoria, Victoria, BC, Canada, ⁴ Department of Biochemistry and Microbiology, University of Victoria, Victoria, BC, Canada, ⁵ Proteomics Centre, Segal Cancer Centre, Lady Davis Institute, Jewish General Hospital, McGill University, Montreal, QC, Canada, ⁶ Gerald Bronfman Department of Oncology, Jewish General Hospital, McGill University, Montreal, QC, Canada

OPEN ACCESS

Edited by:

Duraisamy Saravanakumar,
The University of the West Indies St.
Augustine, Trinidad and Tobago

Reviewed by:

M Loganathan,
Indian Council of Agricultural Research
(ICAR), India
Sivakumar Uthandi,
Tamil Nadu Agricultural
University, India

*Correspondence:

Samina Mehnaz
saminamehnaz@fccollege.edu.pk

Specialty section:

This article was submitted to
Crop Biology and Sustainability,
a section of the journal
Frontiers in Sustainable Food Systems

Received: 11 September 2020

Accepted: 25 January 2021

Published: 22 February 2021

Citation:

Shahid I, Han J, Hanoq S, Malik KA,
Borchers CH and Mehnaz S (2021)
Profiling of Metabolites of *Bacillus*
spp. and Their Application in
Sustainable Plant Growth Promotion
and Biocontrol.
Front. Sustain. Food Syst. 5:605195.
doi: 10.3389/fsufs.2021.605195

Bacillus spp. are well-characterized as efficient bioinoculants for sustainable plant growth promotion and biocontrol of phytopathogens. Members of this spp. exhibit the multifaceted beneficial traits that are involved in plant nutrition and antimicrobial activities against phytopathogens. Keeping in view their diverse potential, this study targeted the detailed characterization of three root-colonizing *Bacillus* strains namely *B. amyloliquefaciens*, *B. subtilis*, and *B. tequilensis*, characterized based on 16S rRNA sequencing homology. The strains exhibited better plant growth promotion and potent broad-spectrum antifungal activities and exerted 43–86% *in-vitro* inhibition of growth of eight fungal pathogens. All strains produced indole acetic acid (IAA) in the range of 0.067–0.147 μM and were positive for the production of extracellular enzymes such as cellulase, lipase, and protease. Ultra-performance Liquid Chromatography-Electrospray Ionization-Mass Spectrometry (UPLC-ESI-MS/MS) analysis revealed the production of antifungal metabolites (AFMs) such as surfactins, iturins, fengycins, macrolactins, bacillomycin-D, and catechol-based siderophore bacillibactin which were further confirmed by amplifying the genes involved in the biosynthesis of these antimicrobial lipopeptides. When compared for the amounts of different cyclic-peptides produced by three *Bacillus* strains, *B. amyloliquefaciens* SB-1 showed the most noticeable amounts of all the antifungal compounds. Plant experiment results revealed that inoculation with phytohormone producing *Bacillus* spp. strains demonstrated substantial growth improvement of wheat biomass, number of spikes, and dry weight of shoots and roots. Results of this study indicate the biocontrol and biofertilizer potential of *Bacillus* spp. for sustainable plant nutrient management, growth promotion, and effective biocontrol of crop plants, particularly cultivated in the South Asian region.

Keywords: biopriming, *Bacillus amyloliquefaciens*, cyclic-lipopeptides, mass spectrometry, siderophores, biofertilizer

INTRODUCTION

Increasing environmental concerns and food safety issues gave momentum to the use of bio-fertilizers and biological control agents in agriculture sector world-wide. Moreover, to combat the threatening challenges of non-degradable and recalcitrant agrochemicals, and increased pesticide resistance, plant growth promoting bacteria (PGPB), and their bioactive metabolites got global attention (Bhardwaj et al., 2014). PGPB exert multifaceted benefits to the plants and enrich soil nutrients by means of phosphate/potassium/zinc mineralization, release of plant growth promoting regulators and hormones, and nitrogen fixation (Hayat et al., 2010; Saharan and Nehra, 2011). Furthermore, their contribution in plant defense through the production of metabolites make them significant and key players in sustainable agriculture (Sinha et al., 2014).

Currently, main plant growth promoting rhizobacteria (PGPR) include *Azotobacter*, *Azospirillum*, and *Rhizobium* [N₂-fixers], *Gluconacetobacter*, *Enterobacter*, *Azoarcus*, *Klebsiella*, *Burkholderia*, *Pantoea*, *Stenotrophomonas* spp. [mineral mobilizers and plant-hormone regulators], *Bacillus* and *Pseudomonas* [PGP and biocontrol agents]. Among these predominant and the most widely studied are *Bacillus* and *Pseudomonas* spp. for their characteristic roles in nutrient acquisition and assimilation, secretion and modulation of hormones, plant beneficial secondary metabolites, antifungal metabolites (AFMs), antibiotics, and various extracellular signaling compounds (Ahemad and Kibret, 2014; Agler et al., 2016). *Bacillus* spp. have been in limelight for their long shelf-life in bio-formulations, effective colonization of plant tissues, and broad-spectrum antifungal abilities (Souza et al., 2014). Almost 4–5% genome of *Bacillus* spp. is dedicated for the production of structurally diverse antimicrobial compounds that have demonstrated varying antagonism against fungal and bacterial phytopathogens. Most significant among these antimicrobials are cyclic-lipopeptides (CLPs) constituting iturins, fengycins, and surfactins that are pivotal in root colonization by *Bacillus* spp. (Aira et al., 2010; Carvalhais et al., 2013).

Many research studies have investigated the biofertilizer and biocontrol potential of *Bacillus* spp., however, less is known about the complete metabolomic profile, account of the plant growth-promoting traits, secondary metabolites and their variants produced by a single strain. For instance, endophytic *B. subtilis* strain ALB629 was evaluated for its plant growth-promoting traits but its antagonistic secondary metabolites were not identified (Falcão et al., 2014). Likewise, PGPB *Bacillus* strains RM-2 and BPR7 were evaluated for *in-vitro* antagonistic activities, nonetheless, they were not subjected to detailed characterization of their secondary metabolites (Kumar et al., 2012; Minaxi et al., 2012; Shobana et al., 2020).

The following study aimed to identify antifungal *Bacillus* spp., characterization and relative quantification of their strain-specific antagonistic metabolites, and analysis of their biofertilizer potential. Based on the biocontrol potential, three *Bacillus* spp. isolates, i.e., SB-1, A-2, A-3, were hypothesized to be active against phytopathogens of important economic crops and subjected to detailed characterization. Antagonistic metabolites of these isolates were comprehensively documented using

polyphasic approach with the identification of putative genes involved in the production of these metabolites. Furthermore, bacterial isolates were screened for their plant growth-promoting (PGP) traits and their effects as bioinoculants for wheat were evaluated *in-vivo* to be used as multifaceted biofertilizer and biopesticides for various crop plants.

MATERIALS AND METHODS

Isolation and Screening of Bacterial Isolates With Antagonistic Activity

Bacteria were isolated from sugarcane, rice (Lahore, Pakistan, 31.5204° N, 74.3587° E), and corn (Kasur, Pakistan, 31.1179° N, 74.4408° E), using standard serial dilution plating (Somasegaran and Hoben, 1985, **Supplementary Tables 1–3**). Pure bacterial cultures were obtained by streaking single colonies on Luria-Bertani (LB) agar plates incubated at 37°C for 48 h. Antagonistic activity of bacterial isolates was checked against fungal phytopathogens (diseases, affected crops, host plants are described in **Supplementary Table 4**) including *Aspergillus niger* (NCBI accession no. MN786323), *A. flavus*, *Fusarium oxysporum* (NCBI accession no. MN636869), *F. moniliforme* (NCBI accession no. MN636870), *F. solani*, *Colletotrichum falcatum*, *Curvularia* sp. (NCBI accession no. MN636871), and *Rhizopus* sp. (NCBI accession no. MN636450), using plate bioassays. Fungal cultures were obtained from the culture collection of Mycology Laboratory, Forman Christian College (A Chartered University) Lahore, Pakistan and maintained on potato-dextrose agar (PDA) plates at 26–28°C.

In-vitro Inhibition of Mycelial Growth of Pathogens by *Bacillus* spp.

Dual culture assay described by Sakthivel and Gnanama-nickam (1986) was used to determine the antagonistic activity of bacterial isolates against fungal phytopathogens. In a complementary antagonistic experiment, agar well-diffusion assay was performed (Magaldi et al., 2004). Results were expressed as percentage inhibition zones by antagonistic bacteria to suppress the growth of fungal mycelia. Each experiment was performed twice in triplicates and percentage inhibition was calculated as

$$I = (C - T/C) \times 100$$

Where

I = % inhibition, C = fungal diameter in control plate, T = fungal diameter in test plate.

Biochemical and Molecular Characterization of *Bacillus* Isolates

Based on antifungal activity, three bacterial isolates [SB-1 (sugarcane), A-2 (rice), and A-3 (corn)] were selected for detailed studies. These isolates were biochemically characterized using QTS-24 bacterial identification kits (DESTO Laboratories, Karachi, Pakistan) using manufacturer's protocol. Bacterial DNA was isolated using GeneJET genomic DNA purification kit (Thermo Fisher Scientific, USA, catalog number: K0721). 16S rRNA gene was amplified from genomic DNA of isolates SB-1, A2, and A3. Primers and PCR conditions are described in

TABLE 1 | PCR conditions used for amplification of genes from *Bacillus* spp. Isolates.

| Gene/Antibiotic | Target genes | Primers sequences | PCR Profile (35 cycles each) | Amplicon Size (bp) | References |
|-----------------|---|---|--|--------------------|---------------------|
| 16S rRNA | <i>FGPS 1509-153</i> <i>FGPS 4-281</i> | 5'-AAGGAGGTGATCCAGCCGCA-3' 5'-AGAGTTTGATCCTGGCTCAG-3' | Denaturing: 95°C 2 min Annealing: 55°C 60 s Extension: 72°C 90 s Final Extension: 72°C 10 min | 1,500 | (Normand, 1995) |
| Surfactin | <i>sfp-f</i> <i>sfp-r</i> | 5'-ATGAAGATTTACGGAATTTA-3' 5'-TTATAAAAGCTCTTCGTACG-3' | Denaturing: 94°C 1 min. Annealing: 55°C 60 s Extension: 72°C 60 s Final Extension: 72°C 10 min | 675 | (Kefi et al., 2015) |
| Iturin A | <i>ituD-f</i> <i>ituD-r</i> | 5'-ATGAACAATCTTGCCTTTTTA-3' 5'-TTATTTTAAATCCGCAATT-3' | Denaturing: 94°C 3 min Annealing: 55°C 60 s Extension: 72°C 90 sec. Final Extension: 72°C 10 min. | 1,200 | |
| Fengycin | <i>fenD-f</i> <i>fenD-r</i> | 5'-CCTGCAGAAGGAGGAGGACTGAAG-3' 5'-TGCTCATCGTCTCCGTTTC-3' | Denaturing: 94°C 3 min Annealing: 58°C 60 s Extension: 72°C 60 s Final Extension: 72°C 10 min | 300 | (Kim et al., 2010) |
| Bacillomycin D | <i>bmy-f</i> <i>bmy-r</i> | 5'-TGAACAAGGCATATGCTC-3' 5'-AAAATGCATCTGCCGTTCC-3' | Denaturing: 94°C 3 min Annealing: 55°C 60 s Extension: 72°C 60 s Final Extension: 72°C 10 min | 375 | |

Table 1. A reaction mixture of 50 μ L was prepared by using Taq buffer 5 μ L (10X), $MgCl_2$ 2 μ L (25 mM), Taq polymerase (5 U) 2 μ L, dNTPs 2 μ L (2.5 mM), each of forward and reverse primer (20 pmol) 1 μ L, dH_2O 35 μ L, and the template DNA 2 μ L (>50 ng/ μ L). All PCR reagents were purchased from Fermentas (Thermo Fisher Scientific, USA). PCR products were purified using GeneJET PCR purification kit (Thermo Fisher Scientific, USA, catalog number: K0701) and sequenced with both, forward and reverse primers, by Eurofins Genomics, USA. Amplified sequences were compared with NCBI GenBank sequence database, using BLAST search tool and phylogenetic analysis was performed using MEGA5 platform (Tamura et al., 2011). Nucleotide sequences of isolates SB-1, A2, and A3 were aligned with Clustal X 2.1 program. Bootstrap confidence analysis was performed on 1,000 replicates to determine the reliability of the distance tree topologies obtained. The evolutionary distances were computed using the Maximum Composite Likelihood method and are in the units of number of base substitutions per site. All positions containing gaps and missing data were eliminated from the dataset (complete deletion option).

Identification and Pseudo-Relative Quantification of Secondary Metabolites by Ultra Performance Liquid Chromatography- Tandem Mass Spectrometry (UPLC-MS/MS) Extraction of Secondary Metabolites

To identify secondary metabolites, bacterial isolates were individually inoculated to 100 mL LB broth and incubated at 37°C for 48 h in shaking incubator at 180 rpm. Bacterial cultures

were pelleted by centrifugation ($3,900 \times g$ and 4°C for 20 min) and the pH of the supernatants was adjusted to 2.0 with 6N HCl. Secondary metabolites were precipitated by incubating the supernatants overnight at 4°C. The precipitates were recovered by centrifugation ($3,900 \times g$ and 4°C for 20 min) and dissolved in 5 mL of methanol: H_2O (2:1, v/v). The extracts were re-centrifuged ($3,900 \times g$ and 4°C for 20 min), supernatants were dried under vacuum and, re-suspended in 2 mL of methanol, and 10 μ L were injected for each LC-MS analysis.

LC-MS/MS and Data Analyses

Sample solutions were injected onto an Eclipse Plus C18 RRHD column (2.1 \times 100 mm, 1.8 μ m; Agilent, Santa Clara, CA, USA) and separated by reversed-phase liquid chromatography using a Waters Acquity UPLC system (Milford, MA, USA) at a flow rate of 0.4 mL/min. The UPLC system was coupled to an Orbitrap Fusion Tribrid mass spectrometer (Thermo Fisher Scientific, San Jose, CA, USA) equipped with an EASY-Max NG electrospray ion source. The mobile phases were water/0.01% formic acid (A) and 100% acetonitrile/0.01% formic acid (B). Secondary metabolites were separated on the column with a 20 min binary solvent elution gradient (0 min, 5% B; 0–15 min, 5–100% B; 15–17 min, 100% B) followed by a 3-min column equilibration at 5% B between injections. The MS parameters were as follows: positive-ion electrospray spray voltage, 3.9 kV; negative-ion electrospray spray voltage, 2.5 kV; capillary temperature, 325°C; S-lens Level, 60%; sheath gas, 50; sweep gas, 1; and auxiliary gas 10. The MS survey scan was carried out over the mass range m/z 100–2,000, with the data recorded in the centroid mode and at a mass resolution of 120 K FWHM (m/z 200), AGC target 4E5, and one microscan with a maximum inject time of 50 ms in the

quadruple isolation mode. A lock mass at m/z 391.28426 from di(2-ethylhexyl) phthalate (a ubiquitous plasticizer) was used for real-time internal mass calibration during the LC-MS runs with the Fourier Transform (FT) MS detection. In the LC-MS/MS runs, the top five most intense ions, with their charge state of 1 and ion counts of $>5,000$ in each survey scan were selected for MS/MS by collision-induced dissociation (CID) in the linear ion trap or by “higher-energy” collisional dissociation (HCD) in the collision cell in the upfront of the C-trap. Other parameters included: activation isolation window, 2 Da; AGC target for MS/MS, 5E4; maximum inject time, 30 ms; activation time, 10 ms; activation Q, 0.25; and normalized collision energy at 35% for the CID operations. Activation isolation window, 2 Da; AGC target for MS/MS, 5E4; maximum inject time, 30 ms; activation time, 10 ms; activation Q, 0.25; and normalized collision energy at 25% were used for the HCD operations. Raw data files were recorded and processed using the XCalibur 4.1.31.9 (Thermo Scientific) software suite. For relative quantification of secondary metabolites produced by *Bacillus* strains, each sample solution was injected in triplicate and the peak areas were normalized. Bar graphs were plotted with error bars to show the analytical standard deviations.

IDENTIFICATION OF GENES ENCODING SECONDARY METABOLITES IN BACILLUS STRAINS

Detection of the genes encoding surfactin, iturin, bacillomycin, and fengycin was done using gene-specific primers. Primers used in this study and PCR conditions are shown in **Table 1**. An individual reaction mixture of 50 μ L was prepared for all the reactions as described above. PCR products were analyzed on 1% agarose gel. The respective bands were excised and purified using a gel extraction kit. PCR products were sequenced (Eurofins) and analyzed using the NCBI BLAST (blastn) and alignment tools.

IDENTIFICATION AND QUANTIFICATION OF INDOLE-3-ACETIC ACID (IAA)

Preparation of Samples

Bacterial cultures were grown in 10 mL of LB medium at 180 rpm and 37°C temperature, supplemented with L-tryptophan (100 mg/L). After 7 days of growth, bacterial cells were centrifuged at $3,900 \times g$ for 30 min (Allegra TM X-22R Centrifuge, Beckman Coulter, California, USA) and the pH of the supernatants was adjusted to pH 2.0 with 6 N HCl. The acidified supernatants were extracted twice with an equal volume (10 mL) of ethyl acetate. After centrifugation at $3,900 \times g$ for 30 min, the upper organic layers were collected, pooled, and evaporated to dryness.

Preparation of Indole-3-Acetic Acid Standard Curve and LC-MS Quantification

The reference standard of indole-3-acetic acid (IAA, $C_{10}H_9NO_2$, monoisotopic neutral mass = 175.0633, Sigma-Aldrich, USA) was dissolved in methanol:chloroform:H₂O [50:25:25, v/v] at 0.25 mM to form stock standard solution (**Supplementary Table 5**). Ten- μ L aliquots of each standard and

sample were injected into the column for the LC-FTMS (Fourier Transform Mass Spectrometry) runs, as described above. The concentrations in the samples were determined from the peak areas of the extracted ion chromatograms of IAA detected at m/z 176.0706 $[M+H]^+$ by interpolation of the linear-regression calibration curve for this compound (**Supplementary Figure 1**).

Detection of Plant Growth Promoting Traits of *Bacillus* spp.

Lipase production was checked on 1% Tween-20 LB agar plates according to the method of Sierra (1957). Pikovskaya agar medium was used for the detection of phosphatase enzyme (Pikovskaya, 1948). Protease production was checked using skim milk agar plates (Alnahdi, 2012). Extracellular cellulase production was checked on 1% (Carboxymethyl Cellulose) CMC-LB agar plates (Kasana et al., 2008). *In-vitro* zinc solubilization was assessed using the method of Sharma et al. (2012). Siderophore production was detected as per O-CAS method (Louden et al., 2011). Qualitative determination of hydrocyanic acid (HCN) production carried out as per alkaline-picric acid method (Millar and Higgins, 1970).

Plant Experiment

In-vivo effect of *Bacillus* spp. as bioinoculants was evaluated using pot experiments in climate control room. Soil used for this experiment was taken (0–50 cm) from wheat field, demonstrated the following physico-chemical properties: temperature (°C) = 21.7, pH = 7.65, moisture (%) = 23, texture = silty loam, electrical conductivity ($EC_{1:1}$ dS/m) = 1.15, organic matter (OM g/kg) = 29.2, and potential acidity (H⁺ Al mg/kg) = 47.3. Soil was sieved and sterilized in drying oven at 90°C overnight, to eliminate native microbial communities and analyzed post-sterilization to determine any microbial population. Pots were filled with 300 g soil (per pot) and 25 mL of half-strength Hoagland’s solution per pot was added (Hoagland and Arnon, 1970). For seed sterilization, 100 seeds of wheat variety, i.e., Faisalabad-2008 were soaked in 100 mL of 0.1 N bleach (sodium hypochlorite; NaClO) solution for 15 min, and given four successive washes of 10 min each with sterile dH₂O (Chen et al., 2018). Seeds were transferred to 1% water-agar plates and incubated at 22–24°C. Three days old germinated seedlings were transferred in pots (1 seed/pot) and inoculated with 1 mL of individual bacterial culture containing 1×10^7 cells/mL in 10 replicates for each treatment. Plants were kept in a climate control room at relative humidity of 60% with a 12 h photoperiod (200 μ M·m⁻²·s⁻¹ at pot heights with fluorescent lights, 15/20°C). The experiment was set up in a completely randomized block design (CRBD). The temperature in climate room was maintained at $20 \pm 2^\circ\text{C}$; with light source of $6,000 \pm 500$ FLUX and light period of 10 ± 1 h. To provide moisture, plants were watered at alternate days using autoclaved distilled water and second dose of half strength Hoagland’s solution was applied after 15 days. Plants were harvested after 50 days, roots were thoroughly washed and the root and shoot lengths of individual plants of each treatment were noted. Roots and shoots were detached to determine fresh weights of roots and shoots following drying in an oven for 72 h at 70°C to record dry weights of shoots and roots.

Statistical Analysis

All the experiments were performed in triplicate and the average of each data was taken. Data was statistically analyzed using the Statistical Package for the Social Sciences (SPSS) software (IBM Statistics 23.0) at $\alpha = 0.05$.

RESULTS

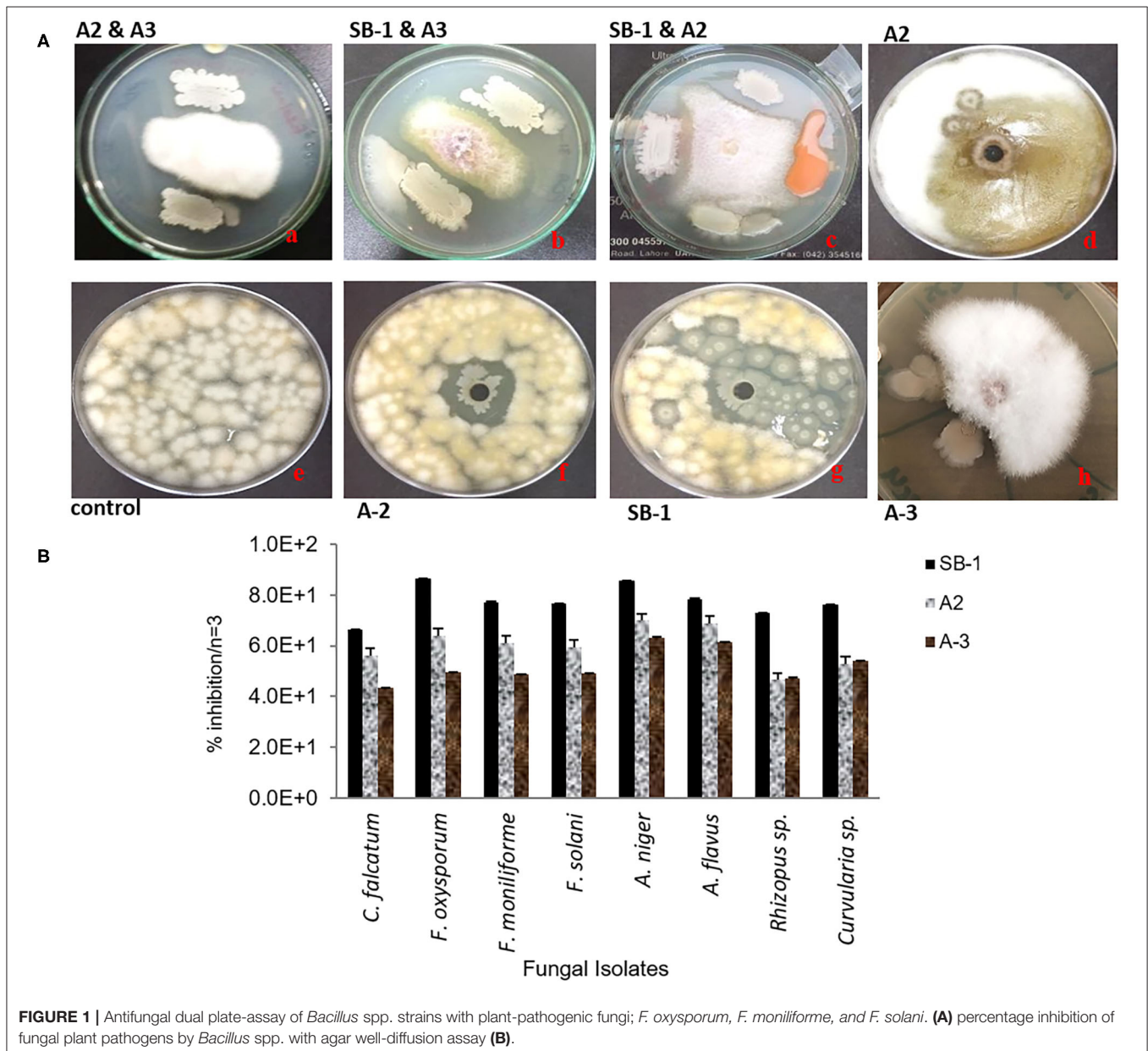
In-vitro Inhibition of Mycelial Growth

Three isolates; SB-1 (sugarcane stem), A-2 (rice rhizosphere), and A-3 (corn rhizosphere) exhibited broad-spectrum *in-vitro* antifungal activities against all the pathogens tested (Figure 1A). SB-1 showed ~86% inhibition of *F. oxysporum*, whereas, *Bacillus* strains A-2 and A-3 exhibited ~64 and ~50% inhibition of *F. oxysporum*, respectively. Figure 1B highlights the variable

growth inhibition of fungal pathogens by the bacterial isolates. Strain SB-1 also demonstrated >70% inhibition of mycelial growth of *F. moniliforme*, *F. solani*, *A. flavus*, *A. Niger*, and *Curvularia* sp. Whereas, 60~65% suppression of these pathogens was shown by strains A-2 and A-3. Minimum inhibition (~43%) was noted for the sugarcane red-rot pathogen *C. falcatum* by the strain A-3, however, SB-1 exhibited ~66% suppression of this pathogen. *Rhizopus* sp. was moderately inhibited by all three strains tested (52~65%).

Biochemical and Molecular Characterization of *Bacillus* Isolates

Bacterial isolates were biochemically characterized using QTS-24 bacterial identification kits (Supplementary Table 6). For 16S rRNA gene, sequence data were searched through

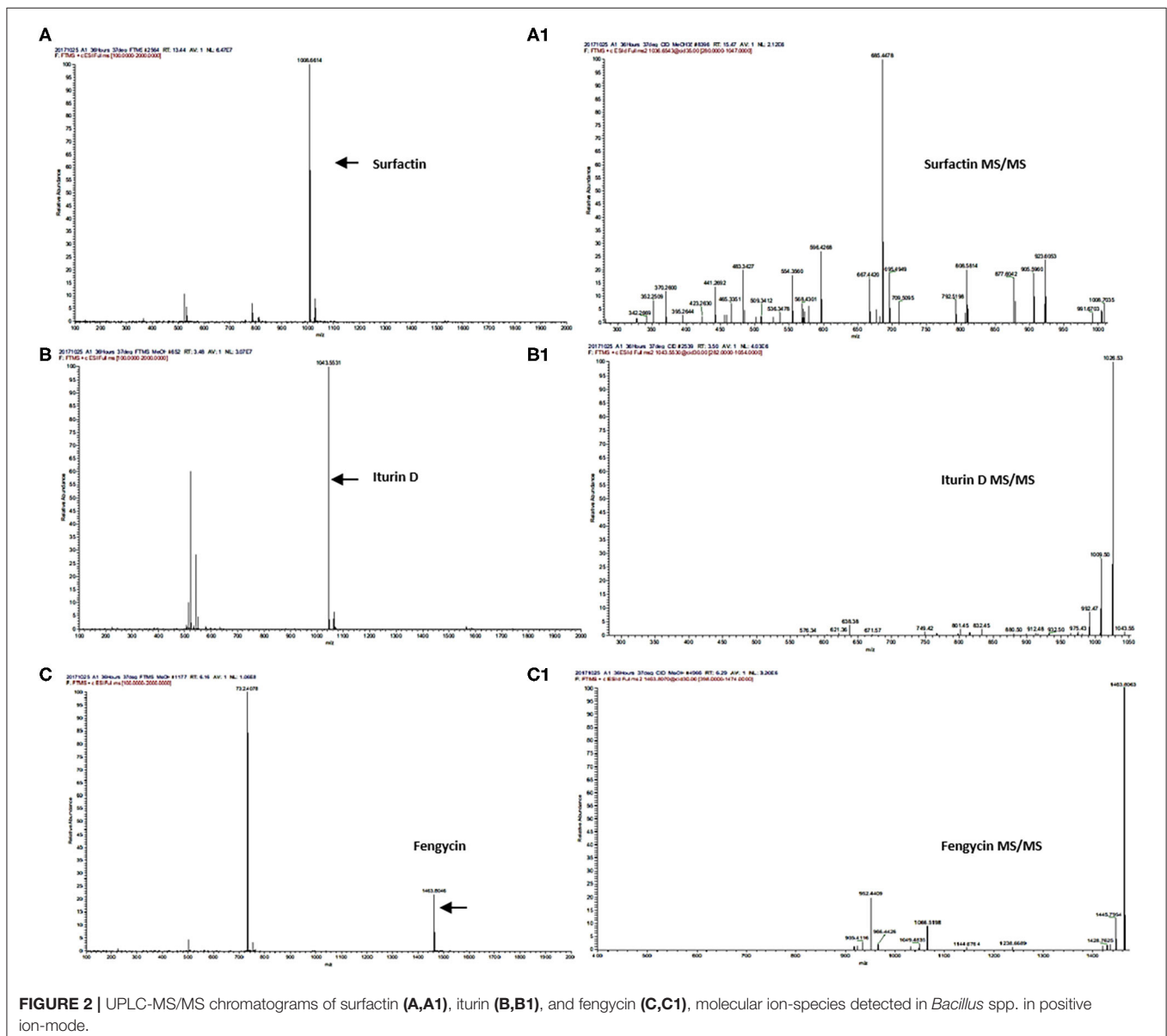


NCBI BLAST. Results confirmed the strain SB-1 as *B. amyloliquefaciens*, and A-2 as *B. subtilis* as they showed 100% homology with 16S rRNA sequences of these strains reported in database. Whereas, strain A-3 exhibited 100% homology with *B. tequilensis* strain (KU179328) and 99.79% homology with *B. subtilis* (KU179327). It was confirmed as *B. tequilensis* due to 99.86 and 99.79% homologies with other reported 16S rRNA sequences of *B. tequilensis* in database (Supplementary Table 7). Phylogenetic tree based on 16S rRNA gene sequences showed the homology of these strains with closely related strains (Supplementary Figure 2). Sequence lengths, accession numbers, and percent homology of each strain are summarized in Supplementary Table 3. There were a total of 1,388 positions in the final dataset of SB-1, 1,387 of A-2 and, 1,362 of A-3. Sequences were deposited in the GenBank database

and accession numbers were obtained (SB-1; MF171193, A-2; MF574398, A-3; MF574399).

Mass-Spectrometry (LC-MS/MS) Analysis and Pseudo-Relative Quantification of Secondary Metabolites of *Bacillus* spp.

Secondary metabolites produced by *Bacillus* strains were first detected by LC/ESI-FTMS in the full-mass scan mode (Figures 3A,B). The first set of peaks observed belong to the surfactin cyclic-lipopeptide (CLPs) family, where strong signals corresponding m/z $[M+H]^+$ were recorded for surfactin C12-C17, i.e., C12 m/z $[M+H]^+$ = 994.644, C13 m/z $[M+H]^+$ = 1008.661, C14 m/z $[M+H]^+$ = 1022.676, C15 m/z $[M+H]^+$ = 1036.692, C16 m/z $[M+H]^+$ = 1050.708, C17 m/z $[M+H]^+$ = 1086.704, produced by all *Bacillus* strains (Figure 2,



Supplementary Figures 3, 5A–K, Supplementary Table 8). Weak signals for sodiated ions $[M+Na]^+$ and deprotonated molecules $[M-H]^-$ of surfactin variants were also recorded. Similarly, peaks for iturin homologs were apparent in both positive and negative ion-modes (**Supplementary Figure 3**). ESI-MS showed strong signals for iturin D $m/z [M+H]^+ = 1043.553$, iturin C $m/z [M+H]^+ = 1044.536$, and iturin A1 $m/z [M+H]^+ = 1029.538$ from *B. amyloliquefaciens* strain SB-1 (**Figure 2, Supplementary Figures 6A–8B, Supplementary Table 8**). The molecular weights of these iturin homologs and their variants were in agreement with iturin structures confirming the acyl chains of C14, C15, C16, and C17. Other than *B. amyloliquefaciens* strain SB-1, *B. subtilis* A-2, and *B. tequilensis* A-3 also demonstrated strong signals for iturin D. However, only weak $[M+H]^+$ signals for iturin A1 and iturin C were recorded for these two strains whereas no $[M-H]^-$ peaks for iturin A1 and iturin C were observed in the extracts of strains A-2 and A-3. Next family of CLPs observed was of fengycin where strong signals corresponding to fengycin $m/z [M+H]^+ = 1463.804$ and fengycin A $m/z [M+H]^+ = 1477.820$ were observed in all three bacterial extracts (**Figure 2, Supplementary Figures 9A–10B, Supplementary Table 8**). Moreover, equally strong sodiated ions $[M+Na]^+$ i.e., fengycin $m/z [M+Na]^+ = 1485.62$ and fengycin A $m/z [M+Na]^+ = 1499.65$ were also noted for this class.

Next strong signals observed in sugarcane endophyte *B. amyloliquefaciens* strain SB-1 corresponded to iturin-like antifungal polypeptide bacillomycin D $m/z [M+H]^+ = 989.494$. Its sodiated ions were not observed, however, weak signals of deprotonated ions were recorded (**Supplementary Figure 11**). Production of bacillibactin, a catechol-based siderophore, was observed in all three *Bacillus* strains. Peaks corresponding to $m/z [M+H]^+ = 883.262$ at retention time of 1.52 were detected in bacterial extracts giving the exact fragmentation pattern of daughter ions, confirming the bacillibactin production (**Figure 2,**

Supplementary Figures 12A,B, Supplementary Table 8). Next two molecular ions detected belonged to bacillaene $m/z [M+H]^+ = 581.358$, and bacilysocin $m/z [M+H]^+ = 471.271$, both of which are polyene and phospholipid antibiotics (**Figure 2, Supplementary Figures 13A–14B, Supplementary Table 8**). Strong signals for bacilysocin were detected in all three strains however, weak signals for bacillaene were observed in strains A-2 and A-3. Besides these, signals for lactone ring harboring macrolide compounds i.e., macrolactin A $m/z [M+H]^+ = 403.247$, macrolactin E $m/z [M+H]^+ = 401.232$, and macrolactin U $m/z [M+H]^+ = 481.331$ were also noted and literature demonstrates their characteristic production from *Bacillus* spp. (**Figure 2, Supplementary Figures 15A–F, Supplementary Table 8**). The MS² fragmentation showed the exact pattern of daughter ions as reported in literature and identified molecules were structurally confirmed by LC-MS/MS. The MS/MS spectra obtained from ion fragmentation in HCD and CID mode were searched against the available MS/MS databases including CFM-ID (Allen et al., 2014), METLIN (Smith et al., 2005), and GNPS (Wang et al., 2016). The MS/MS spectra were also compared with previously published spectra in the literature, especially for those compounds still not entered into any database. Chemical formulas, monoisotopic neutral masses, observed m/z values, and retention times of these compounds have been described in **Table 2**.

All the extracts were analyzed in triplicates following the normalization of peak areas. Average of peak area values were plotted to visualize the comparative amounts of secondary metabolites in three different *Bacillus* strains. Surfactin homologs were abundantly produced by all *Bacillus* strains and amongst them, surfactin C13 $m/z [M+H]^+ = 1008.661$, and C15 $m/z [M+H]^+ = 1036.692$ were observed in high amounts followed by surfactin C14 $m/z [M+H]^+ = 1022.676$ (**Figures 3C–E**). Minimum values were observed for surfactin C17 $m/z [M+H]^+$

TABLE 2 | Chemical formulas, monoisotopic neutral mass, m/z and observed peaks of detected metabolites.

| Sr. No. | Metabolites | Chemical formula | Monoisotopic neutral mass | Monoisotopic m/z | Observed peaks m/z | Retention time | Bacterial strains | | |
|---------|----------------|--|---------------------------|--------------------|----------------------|----------------|-------------------|-----|-----|
| | | | | $[M+H]^+$ | $[M+H]^+$ | | SB-1 | A-2 | A-3 |
| 1 | Surfactin | C ₅₃ H ₉₃ N ₇ O ₁₃ | 1035.683 | 1036.690 | 1036.692 | 14.95 | + | + | + |
| 2 | Iturin A1 | C ₄₇ H ₇₂ N ₁₂ O ₁₄ | 1028.529 | 1029.536 | 1029.538 | 2.57 | + | w+ | w+ |
| 3 | Iturin D | C ₄₈ H ₇₄ N ₁₂ O ₁₄ | 1042.544 | 1043.552 | 1043.553 | 3.48 | + | + | + |
| 4 | Iturin C | C ₄₈ H ₇₃ N ₁₁ O ₁₅ | 1043.528 | 1044.536 | 1044.536 | 3.70 | + | + | + |
| 5 | Bacillibactin | C ₃₉ H ₄₂ N ₆ O ₁₈ | 882.255 | 883.262 | 883.264 | 1.52 | + | w+ | w+ |
| 6 | Bacillaene | C ₃₄ H ₄₈ N ₂ O ₆ | 580.351 | 581.358 | 581.358 | 6.06 | + | + | + |
| 7 | Bacilysocin | C ₂₁ H ₄₃ O ₉ P | 470.264 | 471.271 | 471.271 | 10.06 | + | + | + |
| 8 | Bacillomycin D | C ₄₅ H ₆₈ N ₁₀ O ₁₅ | 988.486 | 989.493 | 989.494 | 1.77 | + | - | - |
| 9 | Fengycin | C ₇₂ H ₁₁₀ N ₁₂ O ₂₀ | 1462.795 | 1463.803 | 1463.804 | 6.16 | + | + | + |
| 10 | Fengycin A | C ₇₃ H ₁₁₂ N ₁₂ O ₂₀ | 1476.482 | 1477.820 | 1477.820 | 6.50 | + | + | + |
| 11 | Macrolactin A | C ₂₄ H ₃₄ O ₅ | 402.240 | 403.247 | 403.247 | 2.82 | + | nd | nd |
| 12 | Macrolactin E | C ₂₄ H ₃₂ O ₅ | 400.189 | 401.232 | 401.232 | 3.25 | + | + | nd |
| 13 | Macrolactin U | C ₃₁ H ₄₄ O ₄ | 480.564 | 481.331 | 481.331 | 10.2 | + | + | + |

nd, not detected; W+, weak positive; +, positive; -, negative.

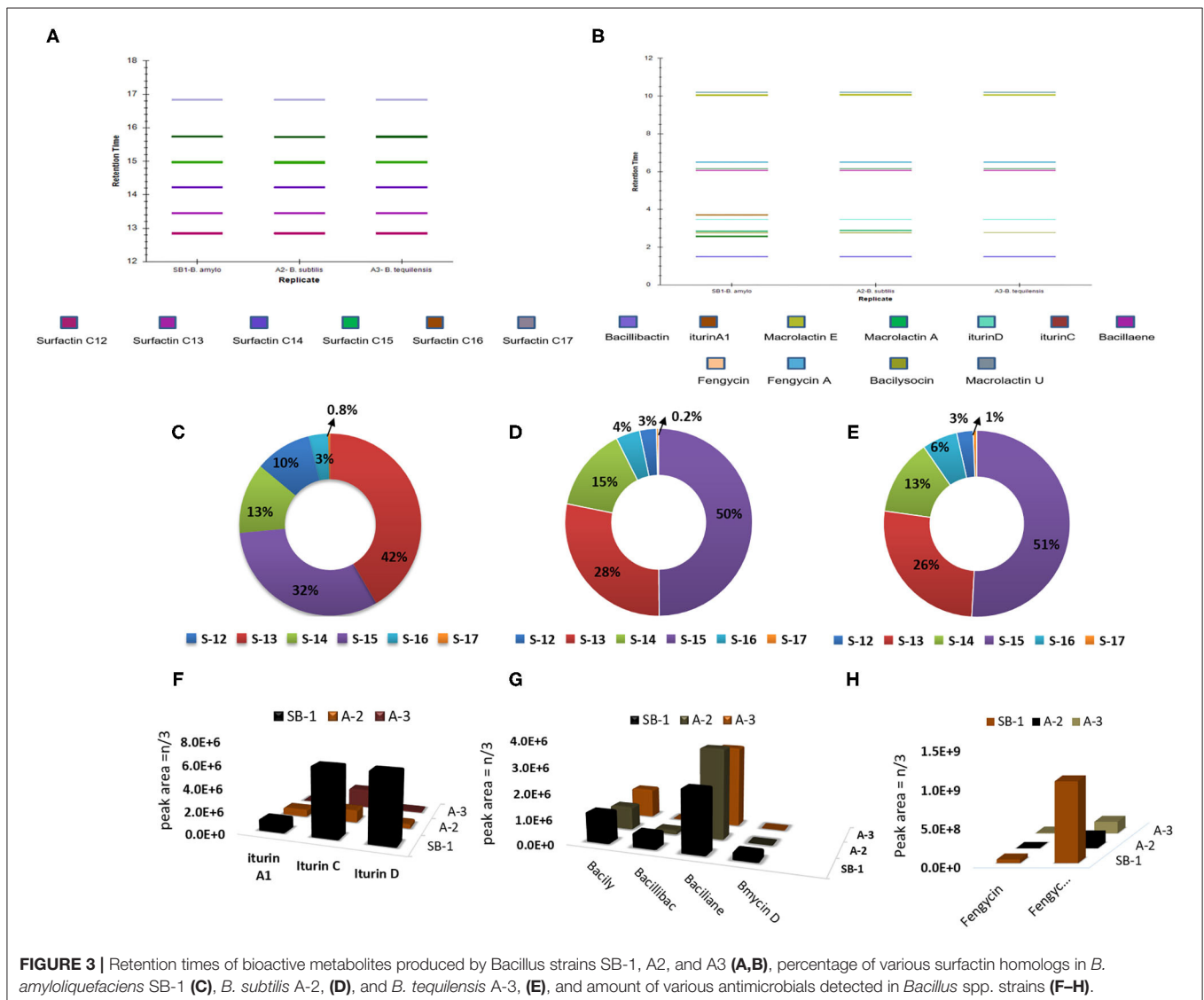
= 1086.704 which contributed 0.2–1% of the total surfactins produced by three strains. Likewise, maximum production of iturin variants was recorded for the strain *B. amyloliquefaciens* SB-1. The Highest amounts were noted for iturin C followed by iturin D in all three *Bacillus* strains, however, very minute amount of iturin A1 was detected for *B. subtilis* A-2 and *B. tequilensis* A-3 (Figure 3F).

Amongst other metabolites, all three *Bacillus* strains produced large amounts of polyene antibiotic bacillaene. Its maximum amount was observed in *B. subtilis* followed by *B. tequilensis* A-3. Moreover, all three strains produced phospholipid-based antibiotic bacilysozin and its production was prominently noted in strains *B. amyloliquefaciens* SB-1 and *B. tequilensis* A-3. Although the production of catechol-based siderophores was noted in all *Bacillus* strains, however, its maximum amount was seen in *B. amyloliquefaciens* SB-1. Production of Iturin-like polypeptide bacillomycin D was nevertheless, variable. Its production was seen only in sugarcane endophyte

B. amyloliquefaciens SB-1 and no peak was recorded with the same mass in other two strains (Figure 3G). *Bacillus* spp. were also compared for the production of cyclic-lipopeptide fengycins and demonstrated high values for fengycin A production. Maximum amounts of fengycin and fengycin A were seen by the strain SB-1 *B. amyloliquefaciens* followed by strains A-3 and A-2 (Figure 3H).

Genes Encoding for Cyclic-Lipopeptides in Bacillus Strains

Gene *sfp* has been reported as the marker for identification of surfactin production by *Bacillus* spp. PCR amplification of *sfp* gene (675 bp) was shown by all three strains. Similarly, *ituD* gene amplification (1,200 bp) was also noted in all three *Bacillus* spp. which is the characteristic biomarker for iturin A production and encodes a putative malonyl coenzymeA transacylase. Amplification of 300 bp fragment with fengycin



primers confirmed that all three *Bacillus* strains harbor the gene for production of fengycin lipopeptide. However, bacillomycin D showed the amplification of 375 bp only in *B. amyloliquefaciens* SB-1 (Figures 4A–D). Moreover, peaks corresponding to bacillomycin D m/z $[M+H]^+ = 989.494$ were only seen in SB-1 confirming that strain A-2 and A-3 do not produce this iturin-like polypeptide. Sequencing of PCR products were searched through BLAST search and confirmed homologies with respective gene sequences reported in database.

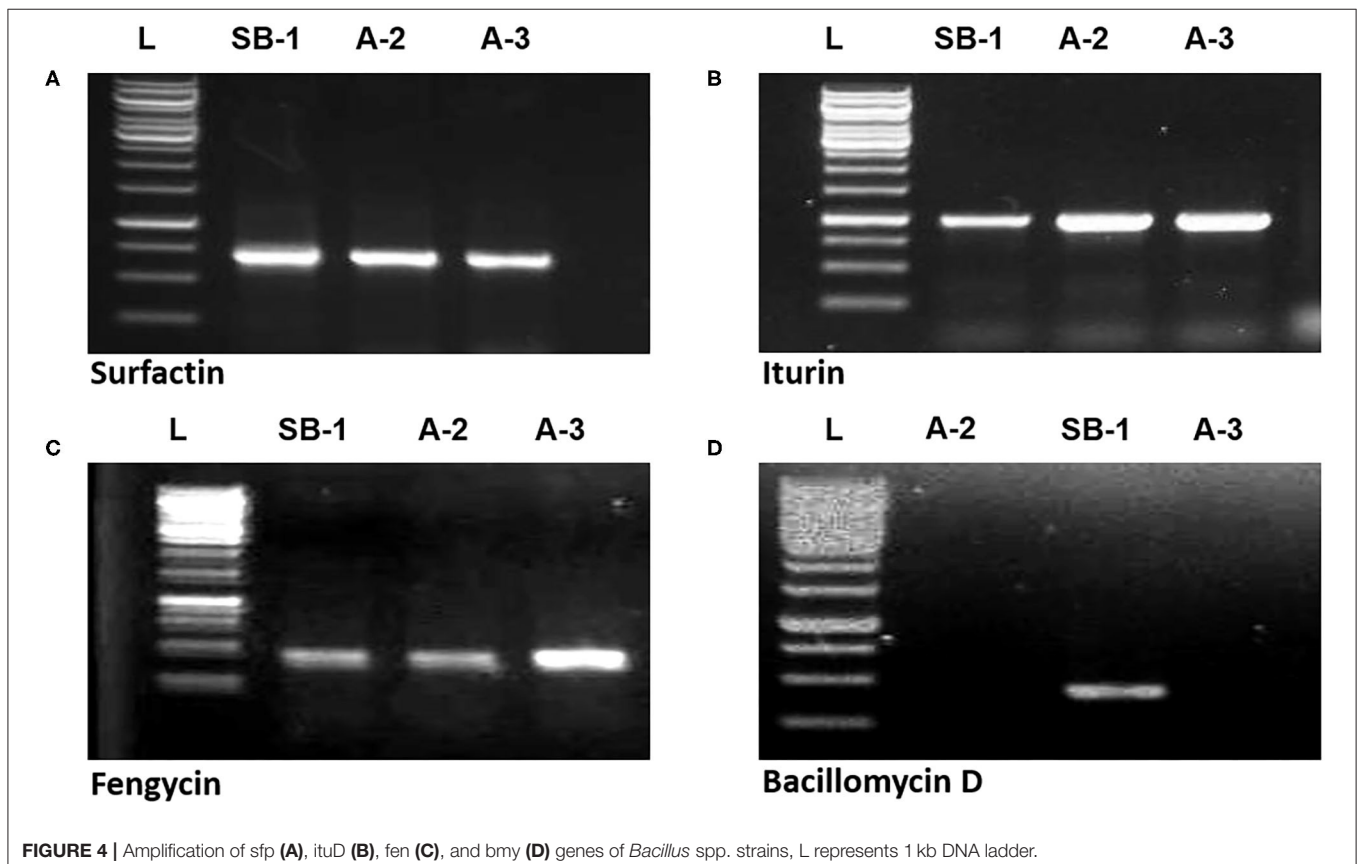
Identification of Plant Growth Promoting Traits of *Bacillus* spp.

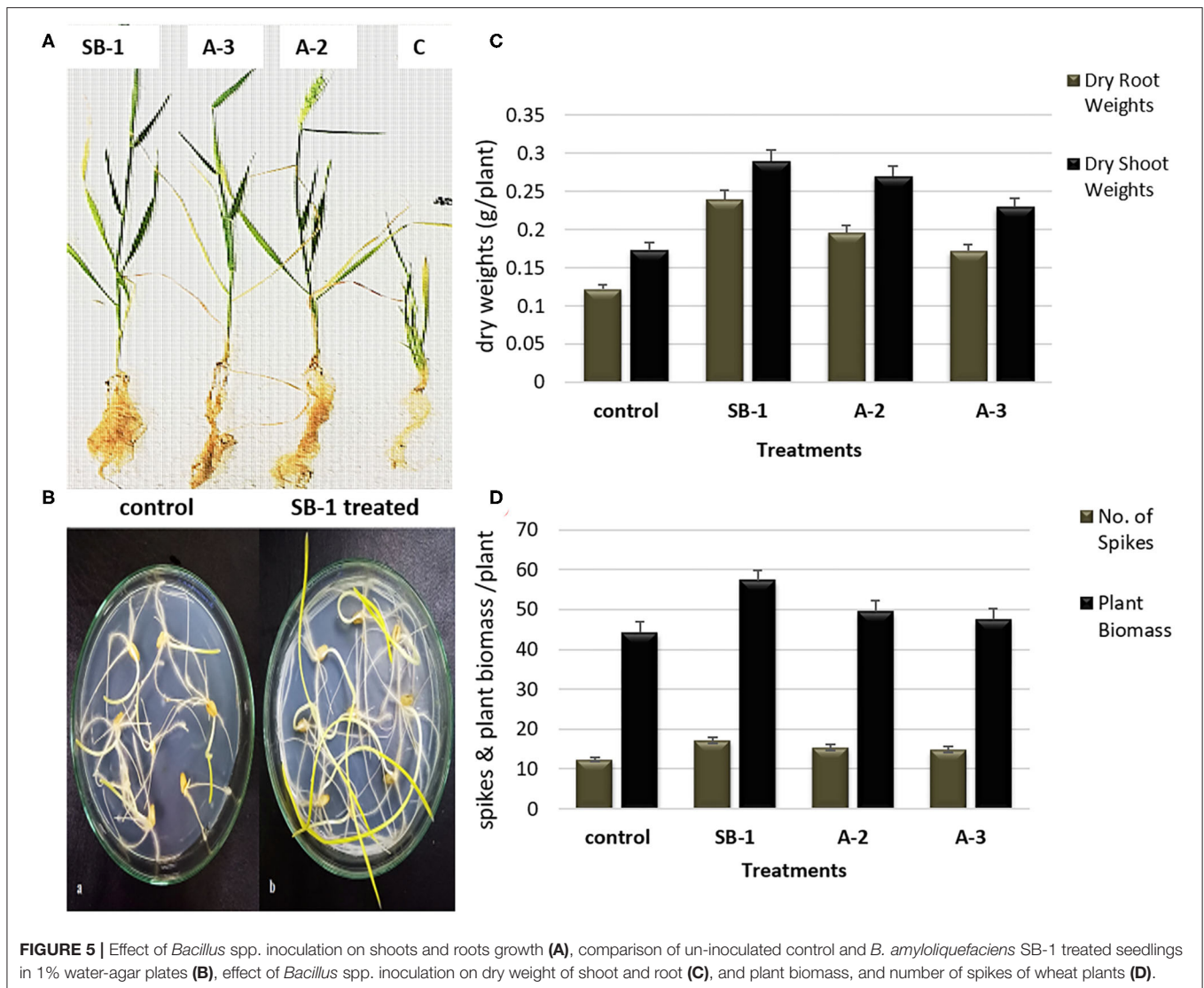
All three *Bacillus* strains produced plant-growth promoting auxin, indole-3-acetic acid. Highest amount of IAA, i.e., $0.147 \mu\text{M}$ was produced by *B. amyloliquefaciens* SB-1 followed by *B. tequilensis* A-3 which produced $0.132 \mu\text{M}$. Least amounts of IAA were noted by *B. subtilis* strain A-2 which produced $0.067 \mu\text{M}$ of IAA. Furthermore, production of extracellular hydrolytic enzymes including protease, lipase, and cellulase was noted by all three *Bacillus* spp. in plate bioassays. None of the strains was positive for volatile HCN production, whereas, all three strains produced catechol-type siderophores in plate bioassays. When checked for insoluble mineral solubilization, only *B. amyloliquefaciens* SB-1 solubilized tris-minimal agar medium supplemented with ZnCO_3 (2.1

± 0.18 SI) and Pikovskya's agar, i.e., $23.2 \pm 0.21 \mu\text{g/mL}$ (Supplementary Table 9).

Stimulation of Wheat Growth by *Bacillus* spp. Bioinoculants

Significant effects of *Bacillus* spp. bioinoculants were noted on the growth of wheat plants. Results manifested that bacterial inoculation stimulated plant growth as compared to the un-inoculated controls. Plants inoculated with *B. amyloliquefaciens* SB-1 demonstrated maximum shoot lengths followed by *B. tequilensis* A-3, and *B. subtilis* A-2, respectively. Maximum root lengths were however noted for *B. subtilis* A-2 inoculated plants followed by *B. tequilensis* A-3 (Figures 5A,B). When compared for dry weights of shoot and root, most significant difference was recorded for the *B. amyloliquefaciens* SB-1 inoculated plants followed by *B. subtilis* A-2. Likewise, *B. amyloliquefaciens* SB-1 substantially increased the overall plant biomass ($\sim 42\%$) as compared to uninoculated controls. *B. subtilis* A-2 inoculated plants were next in the que that showed considerable increase in overall plant biomass ($\sim 31\%$). Although all the inoculated plants demonstrated more spikes in comparison to uninoculated ones, however, *B. amyloliquefaciens* SB-1 inoculated plants were notably significant (Figures 5C,D). Overall results suggested *B. amyloliquefaciens* SB-1 as the most successful bioinoculum for the wheat.





DISCUSSION

Bacillus spp. are omnipresent in nature and constitute a major microbial community of rhizomicrobiome. Root-colonizing *Bacillus* spp. have been extensively characterized for their range of agricultural, environmental, and industrial applications and are regarded as eco-friendly substitutes of chemical fertilizers (Cardinale et al., 2015). Besides possessing diverse plant growth-stimulating factors, *Bacillus* spp. are also bestowed with the immense capacity of producing antimicrobial compounds active against broad range of plant-pathogens. Among these antimicrobials, the most significant are cyclic-lipopeptides which make them versatile tool for phytopathogenic biocontrol (Santoyo et al., 2012; Smith et al., 2017).

This study describes the isolation and polyphasic characterization of three antagonistic *Bacillus* spp. from different plant sources. Based on 16S rRNA sequencing, these strains were characterized as *B. amyloliquefaciens* SB-1, *B.*

subtilis A-2, and *B. tequilensis* A-3. Strain SB-1 showed 100% homology with reported database strains of *B. amyloliquefaciens*. Likewise, rice rhizosphere isolate *B. subtilis* A-2 demonstrated 100% homology with *B. subtilis* KX692273, and 99.93% homology with other reported *B. subtilis* strains accession nos.; KU551205, AB735984, and AY775778. Corn isolate A-3 however, showed 100% homology with one *B. tequilensis* strain (accession no. MF417796) and exhibited 99.79% similarity with two other reported strains of *B. tequilensis* (accession no. KU179328, KU179329). Additionally, this strain showed 99.86% homology with *B. subtilis* strain (accession no. KU179327). Close homologies with two different species can be further resolved with additional biomarkers including DNA-DNA based hybridization. These three *Bacillus* strains demonstrated broad-spectrum *in-vitro* antifungal activities against eight phytopathogens including *F. oxysporum*, *F. solani*, *F. moniliforme*, *C. falcatum*, *A. niger*, *A. flavus*, *Curvularia* sp. and *Rhizopus* sp. Among these, maximum antagonism was observed by

B. amyloliquefaciens SB-1 showing >85% inhibition of *F. oxysporum* and ~60–70% suppression of other fungal pathogens tested. Previous *in-vitro* studies have shown the ability of *Bacillus* spp. in inhibiting the growth of several fungal pathogens. For instance, *B. subtilis* was evaluated for the biocontrol of *C. gloeosporioides* OGC causing anthracnose disease of chili (Luna-Bulbarela et al., 2018). Similarly, *B. subtilis* strain BPR7 isolated from common bean rhizosphere demonstrated antagonism against several plant-pathogenic fungi including *M. phaseolina*, *F. oxysporum*, *F. solani*, *S. sclerotiorum*, and *Colletotrichum* sp. (Kumar et al., 2012). Likewise, *B. amyloliquefaciens* CNU114001 showed effective biocontrol of sclerotinia rot of cucumber fruit (Ji et al., 2013). However, biocontrol potential of *B. tequilensis* have been explored in recent years and one of the latest research studies evaluated the efficacy of *B. tequilensis* strain MML2476 in biocontrol of rhizome-rot disease of turmeric (Chenniappan et al., 2019).

The underlying mechanism of biocontrol of plant diseases (caused by aerial and soil-borne fungi), by *Bacillus* spp. is usually attributed to the production of various antibiotics by this genus. Suppression of plant-pathogenic fungi by *B. amyloliquefaciens* SB-1, *B. subtilis* A-2, and *B. tequilensis* A-3 suggested their secondary metabolites as potential biocontrol agents. When subjected to detailed ESI-LC-MS/MS analysis, all three *Bacillus* spp. strains showed the production of three main classes of cyclic-peptides (CLPs) including surfactins, iturins, and fengycins. These cyclic-lipopeptide bioactive metabolites have been well-evaluated for their biocontrol and pharmaceutical applications. Iturins constitute the group of iturin A~E, bacillomycins, and mycosubtilins which induct ion-conducting pores in the membranes of growing pathogens and damage mycelia (Zhang et al., 2013). Surfactins however, act by membrane disruption and solubilization and considered as the strong bio-surfactants. Many studies illustrate the synergistic effects of surfactins on broadening the biological properties of iturins and where two of them act in a coordinated manner (Fan et al., 2017). Similarly, fengycins have been demonstrated as key factors in antagonism of several *Bacillus* spp. which together with surfactins can elicit induced systemic resistance (ISR) in plants (Fira et al., 2018). Such as, these CLPs were characterized as the major functional bioactive metabolites of *B. amyloliquefaciens* C06 toward suppression of *M. fructicola* (Liu et al., 2011). Likewise, CLPs from *B. amyloliquefaciens* DH-4 were identified as the main antagonizing agents against citrus green mold *P. digitatum* (Chen et al., 2018). UV-MALDI-TOF-MS analysis of bioactive compounds of *B. subtilis* subsp. *subtilis* PGPMori7 revealed iturins, fengycins, and surfactins in triggering the immunity and microbial competition against *M. phaseolina* (Torres et al., 2016). Recently, genomic insights into the endophytic *B. tequilensis* 7PJ-16 strain displayed its biocontrol potential against mulberry fruit sclerotinose (Xu et al., 2019).

The strains *B. amyloliquefaciens* SB-1, *B. subtilis* A-2, and *B. tequilensis* A-3 used in this study, were able to produce various homologs of surfactins, iturins, and fengycin compounds. Well-ionized peaks for surfactin C12-C17, m/z 994.644–1086.704, iturin A1, D, and C, and fengycin were noted in positive ion mode in all strains. Maximum amounts of these CLPs

were however noted for the strain *B. amyloliquefaciens* SB-1 as compared to other two *Bacillus* strains. These homologs were further confirmed through ESI-MS/MS and results were in accordance with previously published mass-spectrometry data for these compounds. Furthermore, the fragmentation patterns of daughter ions were also confirmed by latest databases CFM-ID and GNPS (Smith et al., 2005; Allen et al., 2014). Moreover, amplification of biosynthetic genes responsible for the synthesis of surfactins, iturins and fengycins confirmed the production of these metabolites by the strains under investigation. All strains showed 675 bp amplification for *sfp* gene coding for surfactin, 1.2 kb fragment for iturin D, and 300 bp fragment for fenD. Following amplification, PCR products were sequenced and compared with reported sequences in database.

Surfactins from *B. subtilis* has been evaluated for its role in root-colonization and protection against plant-pathogen namely *P. syringae* in *Arabidopsis thaliana* (Jourdan et al., 2009) and are known for their potential role in initiation of systemic resistance and stimulation of plant-defense (Bais et al., 2004; Hsieh et al., 2004). Likewise, iturin cyclic-peptides are strong antifungal CLPs produced by many of *Bacillus* strains and act by forming small pores in the membranes of the encountering phytopathogens (Zohora et al., 2016; Zhao et al., 2018). Iturins from *B. amyloliquefaciens* and *B. subtilis* were evaluated for effectively managing anthracnose disease of chili caused by *C. gloeosporioides* OGC1 (Ashwini and Srividya, 2014). Similarly, fengycin family homologs have been characterized for suppressing the growth of filamentous fungi by inducing reactive oxygen species (ROS) production and chromatin condensation (Zhang and Sun, 2018). Moreover, Romero et al. (2007) investigated the contribution of iturins and fengycins from four *B. subtilis* strains UMAF6614, UMAF6616, UMAF6639, and UMAF8561 in the suppression of powdery mildew of cucurbits caused by *Podosphaera fusca*.

Furthermore, iturin-like antifungal peptide, bacillomycin D was only detected in *B. amyloliquefaciens* SB-1 and its PCR analysis also revealed the 375 bp product coding for bacillomycin gene. The result was in accordance with LC-MS/MS results which showed the characteristic peak corresponding to bacillomycin m/z [M+H] = 989.494 in the extracts of strain *B. amyloliquefaciens* SB-1 only. Previous research studies manifest the production of bacillomycin D from *B. amyloliquefaciens* and its contribution in inhibiting spore germination. For instance, *B. amyloliquefaciens* strain 83 was extensively investigated for its potential to produce certain bacillomycin D homologs effectively inhibiting fungal spores and mycelia (Luna-Bulbarela et al., 2018). Detailed ESI-LC-MS/MS analysis of *Bacillus* strains also showed the production of a phospholipid- antibiotic, bacilysocin by all strains. Bacilysocin was characteristically reported from *B. subtilis* 168 and was highlighted for its potential competition against other microorganisms during spore germination (Tamehiro et al., 2002). However, genomic insights into the operational group *B. amyloliquefaciens* illustrate the presence of bacilysocin, iron-siderophore bacillibactin, and bacillaene polyene in several strains of *B. amyloliquefaciens*, *B. velezensis*, and *B. siamensis*,

characteristically produced by strains SB-1, A-2, and A-3 in this study (Fan et al., 2017).

Macrolactins produced by *Bacillus* spp. have been demonstrated for their efficient antibacterial properties and were recently found in reshaping the soil bacterial communities (Yuan et al., 2016). Production of macrolides A, E, and U was also noticed by the strains used in this study. *B. amyloliquefaciens* SB-1 showed the presence of all three macrolactin homologs whereas, *B. subtilis* A-2 showed the presence of two macrolactins; E and U. *B. tequilensis* A-3, however, showed the production of only macrolactin U which was further confirmed for its daughter ion fragmentation by MS/MS.

In addition to be efficient biocontrol agents, these strains also manifested to be strong biofertilizer candidates. When screening for plant growth-promoting traits, all strains produced IAA (0.067–0.147 μ M), lipase, cellulase, protease, and catecholate-based siderophore *in-vitro*. Several studies have shown the production these hydrolytic enzymes and siderophores by *Bacillus* spp. (Sayyed et al., 2004; Shaikh and Sayyed, 2014; Jadhav and Sayyed, 2016; Shaikh et al., 2018). Zinc and phosphorous solubilization was however exclusive to *B. amyloliquefaciens* SB-1 which solubilized 23.2 ± 0.21 μ g/mL of insoluble phosphorus and zinc carbonate (SI = 2.1 ± 0.18).

To be used as biofertilizers, the *in-vivo* impact of *Bacillus* spp. inoculation was also investigated in this study on the growth of wheat plants. Substantial increase in the overall wheat biomass, dry roots and shoots weight, and number of spikes was noted for the plants inoculated with *Bacillus* bio-inoculants as compared to un-inoculated controls. The most significant results were shown by *B. amyloliquefaciens* SB-1 as bioinoculant over un-inoculated control plants which caused $\sim 42\%$ increase in the total biomass.

Conclusively, detailed physiological, genetic and metabolomic analyses of three *Bacillus* spp. strains explored their ability as biocontrol and biofertilizer agents. Comprehensive analysis of the secondary metabolites of these strains provided new insights about their adaptation to diverse environmental niches and their strain-specific metabolites. Among these, sugarcane endophyte *B. amyloliquefaciens* SB-1 showed ideal plant growth-promoting and biocontrol abilities and demonstrated all the attributes to be employed as user-friendly, single-strain inoculum. Presumably, its ability to solubilize phosphorous and zinc can convert more elements into the bioavailable forms

to stimulate plant growth and yield. Furthermore, in future, different consortia and single-strains bioinoculum of these plant growth stimulating *Bacillus* spp. can be used for other crops for the competitive suppression of phytopathogens and as biofertilizer agents.

DATA AVAILABILITY STATEMENT

The datasets presented in this study can be found in online repositories. The names of the repository/repositories and accession number(s) can be found in the article/**Supplementary Material**.

AUTHOR CONTRIBUTIONS

IS performed experiments and wrote the manuscript. JH and CB conceptualized the idea. SH helped to prepare illustrations. KM provided workspace. SM edited the manuscript. All authors contributed to the article and approved the submitted version.

FUNDING

This work received financial support from Higher Education Commission (HEC) of Pakistan (Grant No. 1-8/HEC/HRD/2017/7332). The funding was awarded to IS for Ph.D. research work. The metabolomics research at the UVic-Genome BC Proteomics Center was supported by funding to The Metabolomics Innovation Center (TMIC) through the Genome Innovations Network (GIN) from Genome Canada, Genome Alberta, and Genome British Columbia for operations (205MET and 7203) and for technology development (215MET and MC3T) in metabolomics.

ACKNOWLEDGMENTS

The authors would like to thank Dr. Carol E. Parker for assistance with English language editing.

SUPPLEMENTARY MATERIAL

The Supplementary Material for this article can be found online at: <https://www.frontiersin.org/articles/10.3389/fsufs.2021.605195/full#supplementary-material>

REFERENCES

- Agler, M. T., Ruhe, J., Kroll, S., Morhenn, C., Kim, S. T., and Weigel, D. (2016). Microbial hub taxa link host and abiotic factors to plant microbiome variation. *PLoS Biol.* 14:e1002352. doi: 10.1371/journal.pbio.1002352
- Ahemad, M., and Kibret, M. (2014). Mechanisms and applications of plant growth promoting rhizobacteria: current perspective. *J. King Saud Univ. Sci.* 26, 1–20. doi: 10.1016/j.jksus.2013.05.001
- Aira, M., Gómez-Brandón, M., Lázcano, C., Baath, E., and Domínguez, J. (2010). Plant genotype strongly modifies the structure and growth of maize rhizosphere microbial communities. *Soil Biol. Biochem.* 42, 2276–2281. doi: 10.1016/j.soilbio.2010.08.029
- Allen, F., Pon, A., Wilson, M., Greiner, R., and Wishart, D. (2014). CFM-ID: a web server for annotation, spectrum prediction and metabolite identification from tandem mass spectra. *Nucleic Acid Res.* 42, W94–W99. doi: 10.1093/nar/gku436
- Alnahdi, H. S. (2012). Isolation and screening of extracellular proteases produced by new isolated *Bacillus* sp. *J. Appl. Pharm. Sci.* 2, 71–74. doi: 10.7324/JAPS.2012.2915
- Ashwini, N., and Srividya, S. (2014). Potentiality of *Bacillus subtilis* as biocontrol agent for management of anthracnose disease of chilli caused by *Colletotrichum gloeosporioides* OGC1. *3 Biotech.* 4, 127–136. doi: 10.1007/s13205-013-0134-4
- Bais, H. P., Park, S. W., Weir, T. L., Callaway, R. M., and Vivanco, J. M. (2004). How plants communicate using the underground information superhighway. *Trends Plant Sci.* 9, 26–32. doi: 10.1016/j.tplants.2003.11.008

- Bhardwaj, D., Ansari, M. W., Sahoo, R. K., and Tuteja, N. (2014). Biofertilizers function as key player in sustainable agriculture by improving soil fertility, plant tolerance and crop productivity. *Microb. Cell Fact.* 13:66. doi: 10.1186/1475-2859-13-66
- Cardinale, M., Ratering, S., Suarez, C., Zapata, M. A. M., Geissler-Plaum, R., and Schnell, S. (2015). Paradox of plant growth promotion potential of rhizobacteria and their actual promotion effect on growth of barley (*Hordeum vulgare* L.) under salt stress. *Microbiol. Res.* 181, 22–32. doi: 10.1016/j.micres.2015.08.002
- Carvalho, L. C., Dennis, P. G., Fan, B., Fedoseyenko, D., Kierul, K., Becker, A., et al. (2013). Linking plant nutritional status to plant-microbe interactions. *PLoS ONE* 8:e68555. doi: 10.1371/journal.pone.0068555
- Chen, K., Tian, Z., Luo, Y., Cheng, Y., and Long, C. A. (2018). Antagonistic activity and the mechanism of *Bacillus amyloliquefaciens* DH-4 against citrus green mold. *Phytopathol* 108, 1253–1262. doi: 10.1094/PHYTO-01-17-0032-R
- Chenniappan, C., Narayanasamy, M., Daniel, G. M., Ramaraj, G. B., Ponnusamy, P., Sekar, J., et al. (2019). Biocontrol efficiency of native plant growth promoting rhizobacteria against rhizome rot disease of turmeric. *Biol. Control* 129, 55–64. doi: 10.1016/j.biocontrol.2018.07.002
- Falcão, L., Silva-Werneck, J., Vilarinho, B., da Silva, J., Pomella, A., and Marcellino, L. (2014). Antimicrobial and plant growth-promoting properties of the cacao endophyte *Bacillus subtilis* ALB629. *J. Appl. Microbiol.* 116, 1584–1592. doi: 10.1111/jam.12485
- Fan, B., Blom, J., Hans-Peter, K., and Rainer, B. (2017). *Bacillus amyloliquefaciens*, *Bacillus velezensis*, and *Bacillus siamensis* form an “Operational Group B. *amyloliquefaciens*” within the *B. subtilis* species complex. *Front. Microbiol.* 8:22. doi: 10.3389/fmicb.2017.00022
- Fira, D., Dimkić, I., Berić, T., Lozo, J., and Stanković, S. (2018). Biological control of plant pathogens by *Bacillus* species. *J. Biotechnol.* 285, 44–55. doi: 10.1016/j.jbiotec.2018.07.044
- Hayat, R., Ali, S., Amara, U., Khalid, R., and Ahmed, I. (2010). Soil beneficial bacteria and their role in plant growth promotion: a review. *Ann. Microbiol.* 60, 579–598. doi: 10.1007/s13213-010-0117-1
- Hoagland, D. R., and Arnon, D. I. (1970). *The Water-Culture Method for Growing Plants without Soil*. Berkeley, CA: California Agricultural Experimental Station Publications and College of Agriculture, University of California.
- Hsieh, F. C., Li, M. C., and Lin, T. C. (2004). Rapid detection and characterization of surfactin-producing *Bacillus subtilis* and closely related species based on PCR. *Curr. Microbiol.* 49, 186–191. doi: 10.1007/s00284-004-4314-7
- Jadhav, H. P., and Sayyed, R. Z. (2016). Hydrolytic enzymes of rhizospheric microbes in crop protection. *MOJ Cell Sci. Rep.* 3, 135–136. doi: 10.15406/mojcsr.2016.03.00070
- Ji, S. H., Paul, N. C., Deng, J. X., Kim, Y. S., Yun, B. S., and Yu, S. H. (2013). Biocontrol activity of *Bacillus amyloliquefaciens* CNU114001 against fungal plant diseases. *Mycobiology* 41, 234–242. doi: 10.5941/MYCO.2013.41.4.234
- Jourdan, E., Henry, G., Duby, F., Dommès, J., Barthélemy, J. P., Thonart, P., et al. (2009). Insights into the defense-related events occurring in plant cells following perception of surfactin-type lipopeptide from *Bacillus subtilis*. *Mol. Plant Microbe Interact.* 22, 456–468. doi: 10.1094/MPMI-22-4-0456
- Kasana, R. C., Salwan, R., Dhar, H., Dutt, S., and Gulatti, A. (2008). A rapid and easy method for the detection of microbial cellulases on agar plates using gram's iodine. *Curr. Microbiol.* 57, 503–507. doi: 10.1007/s00284-008-9276-8
- Kefi, A., Ben, S. I., Karkouch, I., Rihouey, C., Azaeiz, S., Bejaoui, M., et al. (2015). Characterization of endophytic *Bacillus* strains from tomato plants (*Lycopersicon esculentum*) displaying antifungal activity against *Botrytis cinerea* Pers. *W. J. Microbiol. Biotechnol.* 31, 1967–1976. doi: 10.1007/s11274-015-1943-x
- Kim, P. I., Ryu, J., Kim, Y. H., and Chi, Y. T. (2010). Production of biosurfactant lipopeptides iturin A, fengycin and surfactin A from *Bacillus subtilis* CMB32 for control of *Colletotrichum gloeosporioides*. *J. Microbiol. Biotechnol.* 20, 138–145. doi: 10.4014/jmb.0905.05007
- Kumar, P., Dubey, R. C., and Maheshwari, D. K. (2012). *Bacillus* strains isolated from rhizosphere showed plant growth promoting and antagonistic activity against phytopathogens. *Microbiol. Res.* 167, 493–499. doi: 10.1016/j.micres.2012.05.002
- Liu, J., Zhou, T., He, D., Li, X. Z., Wu, H., Liu, W., et al. (2011). Functions of lipopeptides bacillomycin D and fengycin in antagonism of *Bacillus amyloliquefaciens* C06 towards *Monilinia fructicola*. *J. Mol. Microbiol. Biotechnol.* 20, 43–52. doi: 10.1159/000323501
- Louden, B. C., Haarmann, D., and Lynne, A. M. (2011). Use of blue agar CAS assay for siderophore detection. *JMBE* 12, 51–53. doi: 10.1128/jmbe.v12i1.249
- Luna-Bulbarela, G., Tinoco-Valencia, R., Corzo, G., Kazuma, K., Konno, K., Galindo, E., et al. (2018). Effects of bacillomycin D homologues produced by *Bacillus amyloliquefaciens* 83 on growth and viability of *Colletotrichum gloeosporioides* at different physiological stages. *Biol. Control* 127, 145–154. doi: 10.1016/j.biocontrol.2018.08.004
- Magaldi, S., Mata-Essayag, S., and Hartungde, C. (2004). Well diffusion for antifungal susceptibility testing. *Int. J. Infect. Dis.* 8, 39–45. doi: 10.1016/j.ijid.2003.03.002
- Millar, R., and Higgins, V. J. (1970). Association of cyanide with infection of bird's foot trefoil by *Stemphylium loti*. *Phytopathology* 60, 104–110. doi: 10.1094/Phyto-60-104
- Minaxi, L. N., Yadav, R. C., and Saxena, J. (2012). Characterization of multifaceted *Bacillus* sp. RM-2 for its use as plant growth promoting bioinoculant for crops grown in semi arid deserts. *Appl. Soil Ecol.* 59, 124–135. doi: 10.1016/j.apsoil.2011.08.001
- Normand, P. (1995). Utilisation des séquences 16S pour le positionnement phylétique d'un organisme inconnu. *Oceanis* 21, 31–56.
- Pikovskaya, R. (1948). Mobilization of phosphorus in soil in connection with vital activity of some microbial species. *Mikrobiologiya* 17:e370.
- Romero, D., de-Vicente, A., Rakotoaly, R. H., Dufour, S. E., Veening, J. W., Arrebola, E., et al. (2007). The iturin and fengycin families of lipopeptides are key factors in antagonism of *Bacillus subtilis* towards *Podosphaera fusca*. *Mol. Plant Microbe Interact.* 20, 430–440. doi: 10.1094/MPMI-20-4-0430
- Saharan, B., and Nehra, V. (2011). Plant growth promoting rhizobacteria: a critical review. *Life Sci. Med. Res.* 21.
- Sakthivel, N., and Gnanama-nickam, S. (1986). Toxicity of *Pseudomonas fluorescens* towards rice sheath -rot pathogen *Acrocyndrium oryzae*. *Curr. Sci.* 5, 106–107.
- Santoyo, G., Orozco-Mosqueda, M. D., and Govindappa, M. (2012). Mechanisms of biocontrol and plant growth-promoting activity in soil bacterial species of *Bacillus* and *Pseudomonas*: a review. *Biocont. Sci. Technol.* 22, 855–872. doi: 10.1080/09583157.2012.694413
- Sayyed, A. H., Omar, D., and Wright, D. J. (2004). Genetics of spinosad resistance in a multi-resistant field-selected population of *Plutella xylostella*. *Pesticide Sci.* 60, 827–832.
- Shaikh, S. S., and Sayyed, R. (2014). “Role of plant growth-promoting rhizobacteria and their formulation in biocontrol of plant diseases,” in *Plant Microbes Symbiosis: Applied Facets* ed. N. K. Arora (New Delhi: Springer), 337–351. doi: 10.1007/978-81-322-2068-8_18
- Shaikh, S., Wani, S., and Sayyed, R. (2018). Impact of interactions between rhizosphere and rhizobacteria. *J. Bacteriol. Mycol.* 5:1058.
- Sharma, S. K., Sharma, M. P., Ramesh, A., and Joshi, O. P. (2012). Characterization of zinc solubilizing *Bacillus* isolates and their potential to influence zinc assimilation in soybean seeds. *J. Microbiol. Biotechnol.* 22, 352–359. doi: 10.4014/jmb.1106.05063
- Shobana, N., Thangappan, S., and Uthandi, S. (2020). Plant growth-promoting *Bacillus* sp. cahoots moisture stress alleviation in rice genotypes by triggering antioxidant defense system. *Microbiol. Res.* 2:126518. doi: 10.1016/j.micres.2020.126518
- Sierra, G. (1957). A simple method for the detection of lipolytic activity of micro-648 organisms and some observations on the influence of the contact between cells and fatty 649 acid substrates. *Antonie Leeuwenhoek* 23, 15–22. doi: 10.1007/BF02545855
- Sinha, R. K., Valani, D., Chauhan, K., and Agarwal, S. (2014). Embarking on a second green revolution for sustainable agriculture by vermi-culture biotechnology using earthworms: reviving the dreams of Sir Charles Darwin. *Int. J. Agric. Health Saf.* 1, 50–64. doi: 10.5897/JABSD.9000017
- Smith, C. A., O'Maille, G., Want, E. J., Qin, C., Trauger, S. A., Brandon, T. R., et al. (2005). METLIN: a metabolite mass spectral database. *Ther. Drug Monit.* 27, 747–751. doi: 10.1097/01.fid.0000179845.53213.39
- Smith, D. L., Gravel, V., and Yergeau, E. (2017). Editorial: signaling in the phytomicrobiome. *Front. Plant Sci.* 8:611. doi: 10.3389/fpls.2017.00611
- Somasegaran, P., and Hoben, H. J. (1985). *Methods in Legume-Rhizobium Technology*, Paia. Maui: University of Hawaii NifTAL Project and MIRCEN, Department of Agronomy and Soil Science, Hawaii Institute of Tropical

- Agriculture and Human Resources, College of Tropical Agriculture and Human Resources. Hawaii: Springer. 367.
- Souza, R., Meyer, J., Schoenfeld, R., Costa, P. B., and Passaglia, L. M. P. (2014). Characterization of plant growth-promoting bacteria associated with rice cropped in iron-stressed soils. *Ann. Microbiol.* 65, 951–964. doi: 10.1007/s13213-014-0939-3
- Tamehiro, N., Okamoto-Hosoya, Y., Okamoto, S., Ubukata, M., Hamada, M., Naganawa, H., et al. (2002). Bacilysocin, a novel phospholipid antibiotic produced by *Bacillus subtilis* 168. *Antimicrob. Agents Chemother.* 46, 315–320. doi: 10.1128/AAC.46.2.315-320.2002
- Tamura, K., Dudley, J., Nei, M., and Kumar, S. (2011). MEGA 5: molecular evolutionary genetics analysis using maximum likelihood evolutionary distance, and maximum parsimony methods. *Mol. Biol. Evol.* 28, 2731–2739. doi: 10.1093/molbev/msr121
- Torres, M. J., Pérez Brandan, C., Petroselli, G., Erra-Balsells, R., and Audisio, M. C. (2016). Antagonistic effects of *Bacillus Subtilis* subsp. *subtilis* and *B. amyloliquefaciens* against *Macrophomina phaseolina*: SEM study of fungal changes and UV-MALDI-TOF MS analysis of their bioactive compounds. *Microbiol. Res.* 182, 31–39. doi: 10.1016/j.micres.2015.09.005
- Wang, M., Carver, J. J., Phelan, V. V., Sanchez, L. M., Garg, N., Peng, Y., et al. (2016). Sharing and community curation of mass spectrometry data with global natural products social molecular networking. *Nat. Biotechnol.* 34, 828–837. doi: 10.1038/nbt.3597
- Xu, W., Ren, H., Ou, T., Lei, T., Wei, J. H., Huang, C. S., et al. (2019). Genomic and functional characterization of the endophytic *Bacillus subtilis* 7PJ-16 strain, a potential biocontrol agent of mulberry fruit sclerotinose. *Microb. Ecol.* 77, 651–663. doi: 10.1007/s00248-018-1247-4
- Yuan, J., Zhao, M., Li, R., Huang, Q., Rensing, C., Raza, W., et al. (2016). Antibacterial compounds-macrolactin alters the soil bacterial community and abundance of the gene encoding PKS. *Front. Microbiol.* 7:1904. doi: 10.3389/fmicb.2016.01904
- Zhang, L., and Sun, C. (2018). Fengycins, cyclic lipopeptides from marine *Bacillus subtilis* strains, kill the plant-pathogenic fungus *Magnaporthe grisea* by inducing reactive oxygen species production and chromatin condensation. *Appl. Environ. Microbiol.* 84, e00445–e00418. doi: 10.1128/AEM.00445-18
- Zhang, X., Li, B., Wang, Y., Guo, Q., Lu, X., Li, S., et al. (2013). Lipopeptides, a novel protein, and volatile compounds contribute to the antifungal activity of the biocontrol agent *Bacillus atrophaeus* CAB-1. *Appl. Microbiol. Biotechnol.* 97, 9525–9534. doi: 10.1007/s00253-013-5198-x
- Zhao, H., Xu, X., Lei, S., Shao, D., Jiang, C., Shi, J., et al. (2018). Iturin A-like lipopeptides from *Bacillus subtilis* trigger apoptosis, paraptosis, and autophagy in Caco-2 cells. *J. Cell Physiol.* 234, 6414–6427. doi: 10.1002/jcp.27377
- Zohora, U., Ano, T., and Rahman, M. (2016). Biocontrol of *Rhizoctonia solani* K1 by Iturin A producer *Bacillus subtilis* RB14 seed treatment in tomato plants. *Adv. Microbiol.* 6, 424–431. doi: 10.4236/aim.2016.66042

Conflict of Interest: The authors declare that the research was conducted in the absence of any commercial or financial relationships that could be construed as a potential conflict of interest.

Copyright © 2021 Shahid, Han, Hanoq, Malik, Borchers and Mehnaz. This is an open-access article distributed under the terms of the Creative Commons Attribution License (CC BY). The use, distribution or reproduction in other forums is permitted, provided the original author(s) and the copyright owner(s) are credited and that the original publication in this journal is cited, in accordance with accepted academic practice. No use, distribution or reproduction is permitted which does not comply with these terms.